Ground Support 2023 – J Wesseloo (ed.)

doi:10.36487/ACG_repo/2325_33

Performance in shear of mechanical hybrid rockbolts

G Knox *University of Toronto, Canada*

J Hadjigeorgiou *University of Toronto, Canada*

Abstract

The performance of a rock reinforcement system is a function of successfully matching a rockbolt to ground conditions and the quality of installation. In very heavily fractured ground, the installation of resin or cementitious grouted rockbolts can be challenging. This is due to resin losses within the fractures and voids surrounding the borehole, as well as 'blown out' holes and hole closures. Poor installation can result in quality issues which may prevent a ground support system from achieving its specified performance requirements. In adverse ground conditions, where it is difficult to install grouted rockbolts, a mechanical hybrid rockbolt may provide an alternative.

The typical configuration of a mechanical hybrid rockbolt is a steel tendon mechanically anchored within a friction rock stabiliser. The rockbolt is installed using a percussion force applied by the rockdrill, and the mechanical anchor is subsequently activated using rotation. This installation process improves the rockbolt's resilience to hole closures. The absence of a chemical anchoring medium in this configuration reduces the impact of fractures and voids on the performance of the rockbolt.

Recent work has focused on quantifying the performance of a mechanical hybrid rockbolt when subjected to a pull or impact test. These investigations employed testing configurations where the loading was applied to the thread of the tendon, or the plate affixed to the tendon. Scant information is available on the performance of mechanical hybrid rockbolts when the rockbolt is subjected to either an axial or shear indirect loading case, which are common in fractured rock masses.

This paper describes the methodology and the results of an investigation into the performance of the mechanical hybrid rockbolt when subjected to indirect axial pull testing and shear loading. The investigation was conducted under laboratory-controlled conditions and resulted in consistent and repeatable results.

Keywords: *shear testing, mechanical hybrid rockbolt, laboratory conditions*

1 Introduction

A major challenge in the design of ground support is selecting a system that can adequately perform in the anticipated ground conditions for the service life of an excavation. This requires an understanding of both the demand and the capacity of the ground support system. Although the design process is relatively straightforward for what may be considered 'normal' ground conditions (e.g. static conditions in moderate to good rock mass quality), this is more difficult in 'extreme' conditions (rockburst prone, squeezing ground).

Recent years have seen the introduction of several yielding, or energy-absorbing rock reinforcement elements that can sustain the support resistance over greater displacement when compared to conventional rockbolts. Although the determination of the demand associated with seismic loads remains a challenge (Stacey 2012), there has been significant progress in quantifying the performance of rock reinforcement elements under static and axial impact loading under controlled laboratory conditions. Arguably there is a better understanding of the comparative capacity of the various rockbolts under controlled conditions.

Of equal importance to the specified performance in the ground support design is the ability to install the ground support effectively and efficiently. This can be challenging for the installation of resin grouted rockbolts in stressed, friable and fractured rock. In effect, borehole closures prevent the installation of resin cartridges and fractures surrounding the hole result in resin losses, reducing the quality of the installation

and eroding the capacity of the rock reinforcement element. A consequence of the poor installation is that the rockbolts may fail to meet the desired design capacity.

Knox & Hadjigeorgiou (2023) illustrate some of the QA/QC issues associated with the migration of resin into the fractured rock as illustrated in Figure 1. Resin migration into joints can result in gaps, or voids, along the rockbolt bar, not attaining the full column and partially mixed resin grout. A way to overcome some of these QA/QC installation issues has been presented by Turcotte (2010) using a hybrid bolt, which is essentially a resin rebar installed within a friction rock stabiliser (FRS). Although the hybrid bolt has been relatively successful in foliated rock masses, the multiple steps of the installation method illustrated in Figure 2 are inefficient. The resin capsules are first inserted into the FRS, which is in turn installed into the borehole. Subsequently, the resin rebar is installed through the bore of the FRS. It was observed, however, that the hybrid bolt performed consistently better than FRS and resin grouted rockbolts in foliated ground.

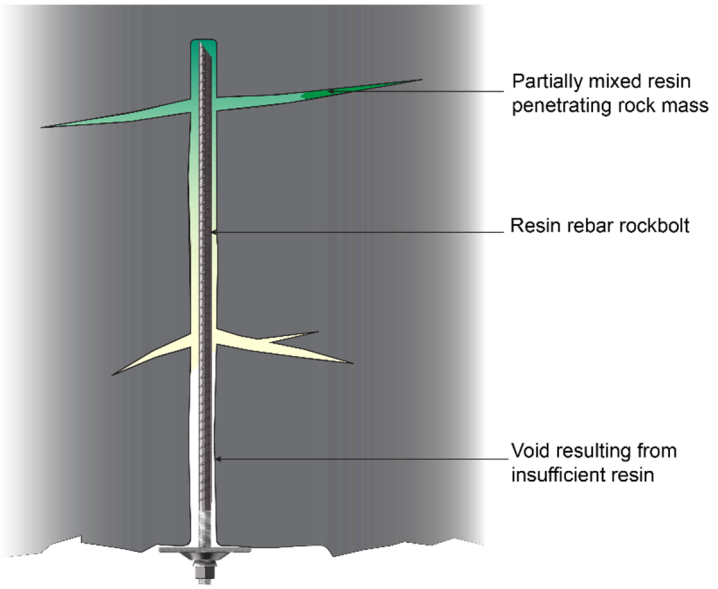

Figure 1 Resin penetration into fractures in the rock mass resulting in failure to achieve a full column bond (Knox & Hadjigeorgiou 2023)

Another reinforcement alternative for poor ground conditions is the use of self-drilling anchors that employ post grouting with a rapid-curing two-component resin. The use of self-drilling anchors overcomes some of the challenges presented by high-stress, fractured and friable rock masses (Watt et al. 2018; Bray et al. 2019; Knox & Hadjigeorgiou 2023). A deterrent in their wide implementation, however, is their relative higher costs and the need for a specialised bolting equipment, e.g. Boltec. Given that mines employ a range of capital equipment for bolting, it is justifiable to explore rockbolt options for poor ground conditions that can be installed using their current equipment fleet.

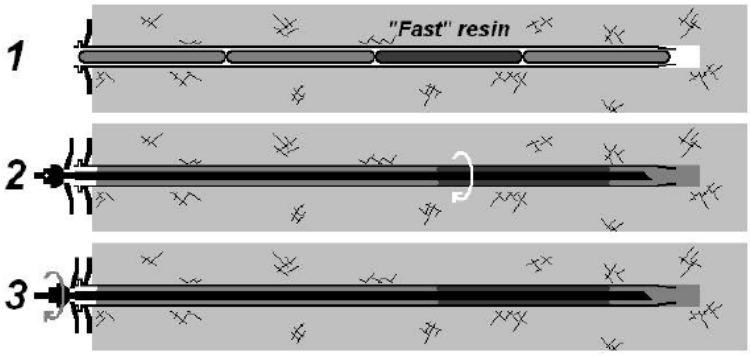

Figure 2 Installation procedure for a hybrid rockbolt (Turcotte 2010)

A second generation of hybrid bolts that do not use resin as part of the reinforcement system is grouped under the heading of mechanical hybrid rockbolts. Andrews (2019) reported the operational benefits of the application of mechanical hybrid rockbolts in highly stressed and fractured masses at two Gold Fields operations: Agnew Mine in Australia and South Deep Mine in South Africa. The operational success of the mechanical hybrid rockbolt was attributed to its robust design and the absence of the requirement for a chemical anchor. A concern is that the absence of a chemical encapsulation may render the bolts inappropriate for long-term applications in corrosive environments.

Rockbolts installed in high-stress, fractured and friable rock masses are subject to a combination of tension, compression, shear and torsion loads under a range of loading rates. An additional complexity are variations in boundary conditions due to the anisotropy of the host rock. Consequently, attempts to fully simulate the loading conditions within a laboratory environment are impractical. Nevertheless, it is recognised that well-designed laboratory testing can provide an environment where a single variable can be controlled and investigated. In addition, the relative performance of different bolt types under the same loading conditions can be assessed.

The performance of a mechanical hybrid rockbolt under impact testing conditions has been well documented (Darlington et al. 2018 & 2019; Roach et al. 2019; Vallati et al. 2022). An impact test is a purely axial tensile loading of a rockbolt. Surprisingly there are no results on the shear capacity of hybrid rockbolts. This is a major concern as both analytical and numerical analysis of the reinforcement action of rockbolts may require the shear capacity of the rockbolts to assess the stability of an excavation.

In reality, there are very limited shear test values for most rockbolts. Consequently, the shear capacity of rockbolts is ignored in most analytical and empirical design approaches. Stjern (1995) conducted a shear test on a Ø46 mm FRS and recorded a shear load (≈160 kN) that exceeded the tensile load (≈60 kN). This was attributed to the difference in the failure mechanism, sliding during axial loading and rupture during shear loading. These tests were conducted using the SINTEF rockbolt pull testing rig in Norway, where the embedment length of the FRS was 980 mm (less than the critical embedment length of the FRS).

Chen & Li (2014) conducted shear tests on paddled energy-absorbing bolts and rebar rockbolts. It was observed that during the investigation, lower shear loads were recorded in comparison to the tensile loads. Knox & Hadjigeorgiou (2023) reported the shear strength of two sets of self-drilling anchor bolts (conventional and energy-absorbing), noting a reduction in the shear load (F_s) when compared to the ultimate tensile load (F_t) for both sets of rockbolts. A greater reduction in the shear load was recorded for the conventional self-drilling anchor ($F_s = 0.81 \times F_t$) compared to the energy-absorbing self-drilling anchor ($F_s = 0.92 \times F_t$).

It is reiterated that that no data has been published on the shear performance of a mechanical hybrid rockbolt. Arguably, the tests from Stjern (1995) on FRS, and Chen & Li (2014) on rebar rockbolts, may provide some insights on how a hybrid bolt (a tendon within the FRS) may behave. This is not supported by any shear tests on mechanical hybrid rockbolts.

This paper describes the methodology and the results of an investigation into the performance of a mechanical hybrid rockbolt when subjected to indirect axial pull testing and shear loading of the rockbolt. The investigation was conducted under laboratory-controlled conditions and resulted in consistent and repeatable results. This constitutes the first set of data on the shear capacity of hybrid bolts of any kind.

2 Mechanical hybrid rockbolt

A typical mechanical hybrid rockbolt, illustrated in Figure 3, consists of a steel tendon mechanically anchored within a FRS. The mechanical anchor consists of a wedge and leaves, with the wedge affixed to the distal end of the tendon within the FRS which becomes the leaves. The frictional interface between the FRS and the perimeter of the borehole provides the initial resistive force against which the wedge is activated through tensioning of the nut. The diameter of the bar is typically maintained while the diameter of the friction unit is selected as either a Ø46 mm or a Ø39 mm, depending on the requirements of the application.

Several suppliers offer variations of a mechanical hybrid rockbolt (DSI Underground 2023; Jennmar 2023; Sandvik 2023; Epiroc 2023). The design and performance specifications vary between the suppliers, however, the key components of the mechanical hybrid rockbolts are similar. This investigation was conducted on Epiroc's the 2.4 m Ø39 mm Vulcan Bolt.

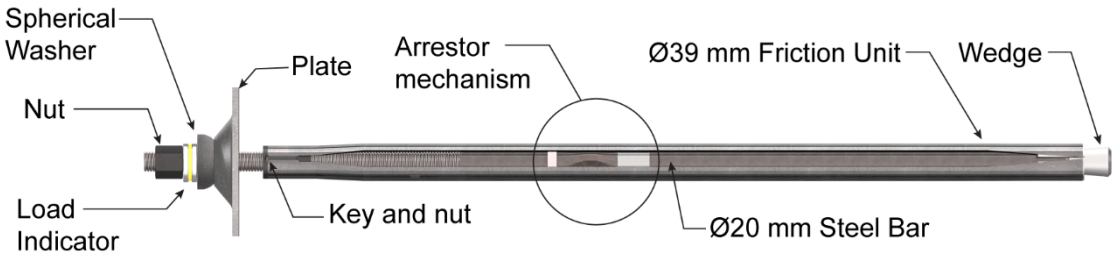

Figure 3 Vulcan Bolt is an example of a mechanical hybrid rockbolt

The installation process for mechanical hybrid rockbolts is illustrated in Figure 4. The first step is drilling of the borehole. The rockbolt is subsequently installed via percussion into the pre-drilled hole (b). The percussive force is applied to the back of the nut using a rockdrill with the rotation disengaged. Once the plate is in firm contact with the rock mass (c), a rotation is applied to the nut (d). The rotation activates the mechanical anchor by pulling the wedge in to the leaves expanding the FRS, completing the installation cycle. The anchorage of the FRS maintains the position of the rockbolt during the activation of the mechanical anchor. This relatively simple installation process can be conducted effectively using a drill rig or a specialised bolting rig.

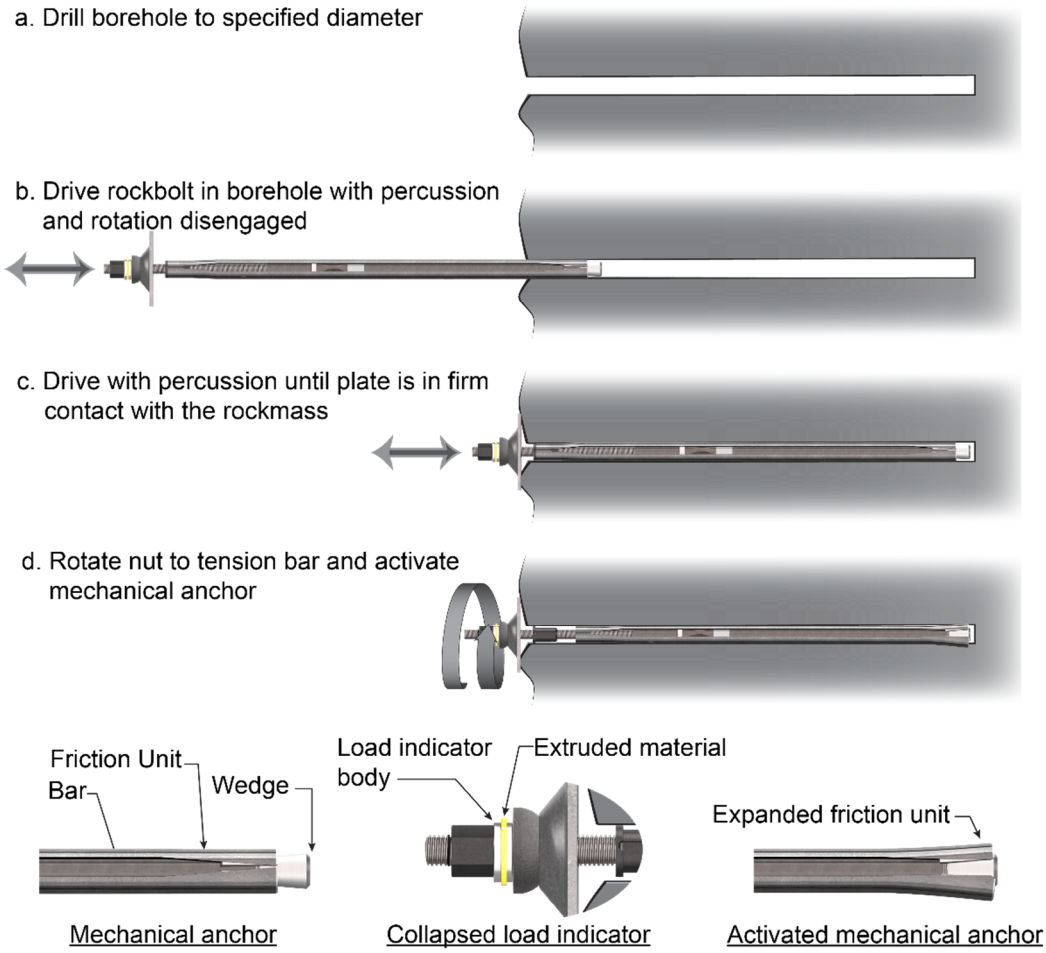

Figure 4 Installation sequence of a mechanical hybrid rockbolt

3 Experimental program

The experimental program aimed at quantifying the tensile and shear capacity of a mechanical hybrid rockbolt. In addition, the relationship between the tensile and shear capacity was of interest, given that ground control engineers often assume a range of shear/tensile ratios for design purposes. The investigation was designed to mitigate the uncertainty of the components of the experiment. In addition, the sourcing of the rockbolts was controlled. This has resulted in a reduction of epistemic uncertainty, and greater confidence in the results.

3.1 Testing apparatus

The investigation was conducted using the Epiroc combination shear and tensile (CST) rockbolt pull tester, seen in Figure 5. The rig configuration followed the SINTEF rig (Stjern 1995), with modifications to the hydraulic control system to accommodate increased sample length and higher shear loading capacity. The CST rockbolt pull tester consists of a loading frame, shear and axial loading trollies, concrete blocks and a hydraulic power pack. Each of the trolleys are driven by two independently controlled hydraulic cylinders equipped with load cells and internal linear variable differential transformers (LVDTs), as illustrated in Figure 6. The testing cycle can be controlled either by the loading or displacement rate. Displacements between the components of the loading train are accounted for using strategically located external LVDTs (see Figure 6). These measurements facilitate the calculation of the displacement of the rockbolt sample. The specifications of the CST equipment are summarised in Table 1.

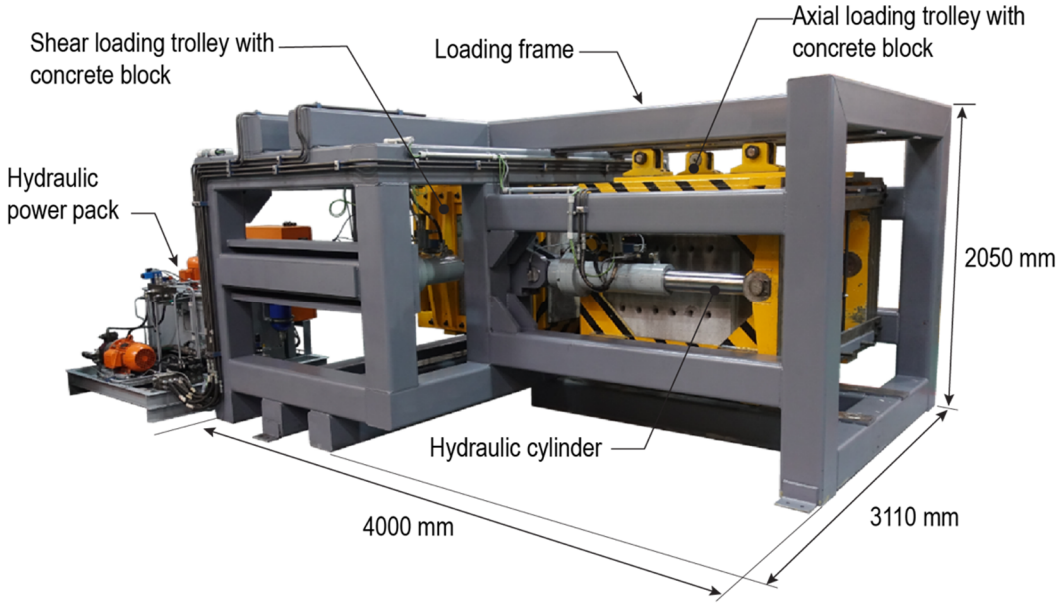

Figure 5 Epiroc combination shear and tensile rockbolt pull tester (Knox & Hadjigeorgiou 2023)

Table 1 Epiroc rockbolt pull tester (Knox & Hadjigeorgiou 2023)

Parameter	Capacity
Shear load (kN)	500
Shear displacement (mm)	300
Tensile load (kN)	500
Tensile displacement (mm)	500
Max. bolt length (mm)	2,400
Bond length (mm)	1,200

As illustrated in Figure 6, the rockbolt is installed through the two concrete blocks (axial and shear loading blocks). During the loading sequence, the load trolleys are driven apart by the hydraulic cylinders. The block translation is controlled by the configured loading profile. This allows for a combination loading that can extend from pure axial (0°) to pure shear loading (90°). During loading, data are recorded at 100 Hz and processed to determine the load–displacement response of the rockbolt.

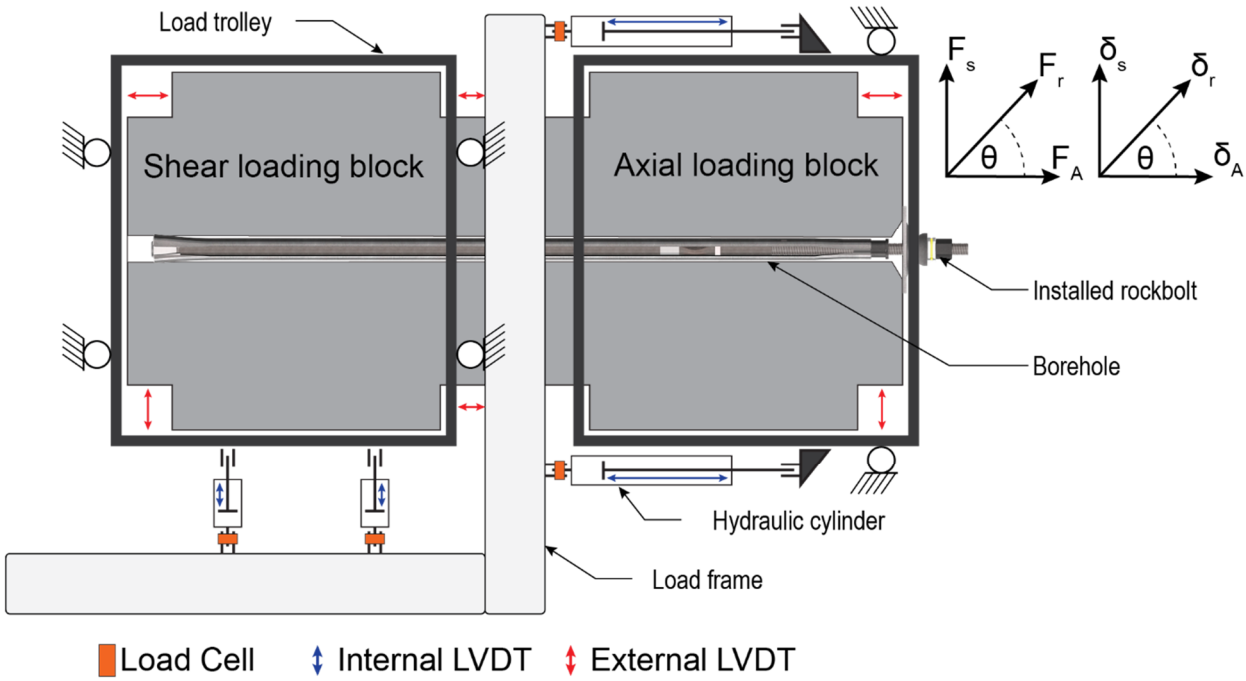

Figure 6 Schematic of the Epiroc combination shear tensile rockbolt pull tester

A shear test under controlled conditions in a laboratory is arguably an index test. Factors such as joint roughness, infilling, lithology and normal pressure can contribute to variations in the shear resistance of a reinforced joint. The aim of this test is to determine the capacity of the rockbolt. Consequently, prior to applying a shear load, a displacement of 3 mm is applied to the axial loading block to ensure a separation between the two blocks. This mitigates the influence of any friction between the blocks in the axial and shear results.

3.2 Sample preparation

The host block material can also influence the shear performance of a rockbolt (Hartman & Hebblewhite 2003). Consequently, significant emphasis was placed on the preparation of the concrete blocks used for the installation of the rockbolts.

The concrete blocks are cast using a mould designed for the profile of the trolleys. Once the pre-mixed concrete has been poured and vibrated to remove air from the mixture, the block is left to cure for a period of 28 days. A centrally located two-by-two-hole pattern spaced at 250 mm between the support holes was drilled using a S25 pneumatic rockdrill (Figure 7a). The support holes were drilled with a Ø38 mm diameter, seven button knock-off bit. The internal profile of the support hole is thus similar to that which is anticipated within the rock mass. The increase of the spacing from 150 mm to 250 mm reduced the borehole breakout observed in the concrete blocks (Knox & Hadjigeorgiou 2023).

The 3,200 kg concrete blocks are installed into the trolleys, aligned, seated and fixed into place to ensure alignment of the hole between the two concrete blocks (Figure 7b). The trolleys are then positioned using the hydraulic cylinders, resulting in a compressive force being applied at the joint. The rockbolt was then installed through the concrete blocks using an Epiroc handheld hydraulic rockdrill (HRD), and manually tensioned with a wrench to activate the mechanical anchor (Figure 7c).

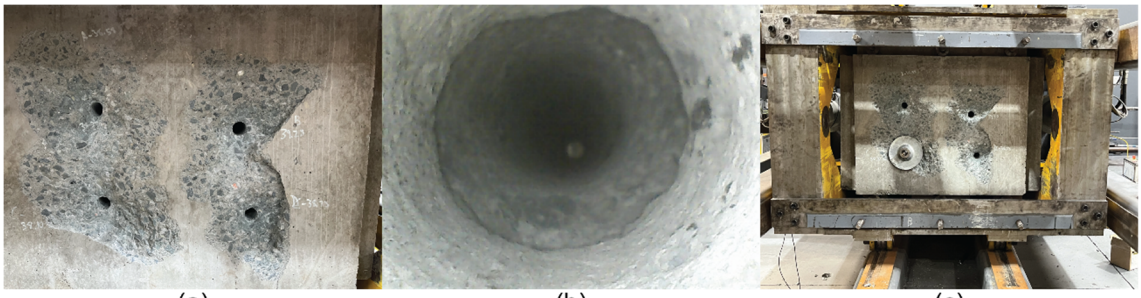

Figure 7 Sample preparation: (a) Support hole pattern and breakout; (b) Alignment of support hole between the two blocks; (c) VB-203924-T03 installed into the CST prior to pull testing

3.3 Loading configurations

For this investigation, the mechanical hybrid rockbolt was subjected to the two loading configurations illustrated in Figure 8: an axial loading case (a) and shear loading (b). The width of each block installed into the testing rig is 1,200 mm, which constitutes the effective bond length of the sample when installed. For both axial and shear loading cases the rockbolt is installed through both blocks. During the axial loading case the load is then applied to the axial loading concrete block, resulting in separation of the two blocks at the joint. The load response of the rockbolt is recorded in relation to the separation of the concrete blocks.

During shear loading the axial loading block is translated to result in a 3 mm separation between the concrete blocks. The force is then applied to the shear loading block, with the position of the axial loading block maintained throughout the loading cycle. The load response of the rockbolt is recorded in relation to the translation of the shear loading concrete block.

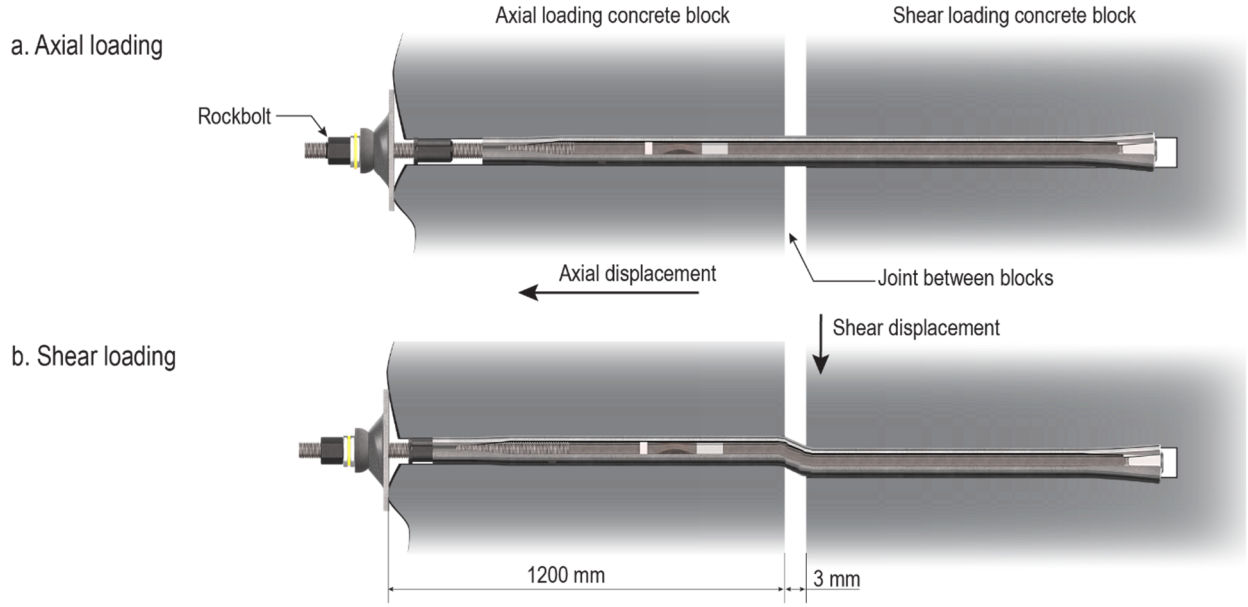

Figure 8 Illustration of the axial and shear loading of the mechanical hybrid rockbolt

4 Experimental results

During this investigation a total of six mechanical hybrid rockbolts were installed and tested to destruction. Three were loaded in direct shear (VB203924-S01 to S03) and three axially (VB203924-T01 to T03). The results of the testing program are summarised in Table 2. For consistency with other tests described by Knox & Hadjigeorgiou (2023), the recorded parameters are illustrated on the load–displacement curve shown in Figure 9.

Table 2 Summary of the axial and shear test results

Sample reference	Loading angle	$\delta_{A_{UF}}$ (mm)	$F_{A_{max}}$ (kN)	$\delta_{s_{UF}}$ (mm)	$F_{s_{max}}$ (kN)
VB203924-T01	0°	252	222	–	–
VB203924-T02	0°	260	224	–	–
VB203924-T03	0°	226	220	–	–
VB203924-S01	90°	–	–	136	307
VB203924-S02	90°	–	–	131	359
VB203924-S03	90°	–	–	206	370

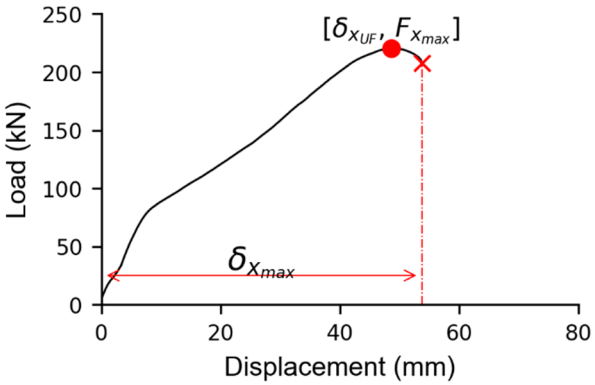

Figure 9 Illustration of the recorded parameters (Knox & Hadjigeorgiou 2023)

The profile of the load–displacement responses for both the shear and axial loading is shown in Figure 10. It should be noted that while the hole size used (Ø38.2 mm) is beyond the upper limit of what is acceptable for a Ø39 mm FRS, this hole size was selected to ensure successful installation using handheld equipment. Consequently, the friction resistance generated during axial loading did not exceed the capacity of the friction unit, resulting in a sliding failure mechanism of the frictional interface observed and depicted in Figure 11. At displacements beyond the rupture of the tendon, the frictional resistance recorded was negligible and the test was terminated.

The host material is a component of the shear loading mechanism. The concrete pre-mix provides a relatively consistent and homogeneous medium, minimising variability in the results. Prior to shear loading an axial load is applied to the tendon to ensure that the two concrete blocks are separated. Consequently, the recorded shear response is entirely attributed to the resistance offered by the mechanical hybrid rockbolt. The additional shear resistance is a consequence of both the tendon and the FRS being loaded, which is evident by the fact that both elements of the rockbolt ruptured in shear. This is different to what was observed during the axial loading process, where only one element (the tendon) ruptured.

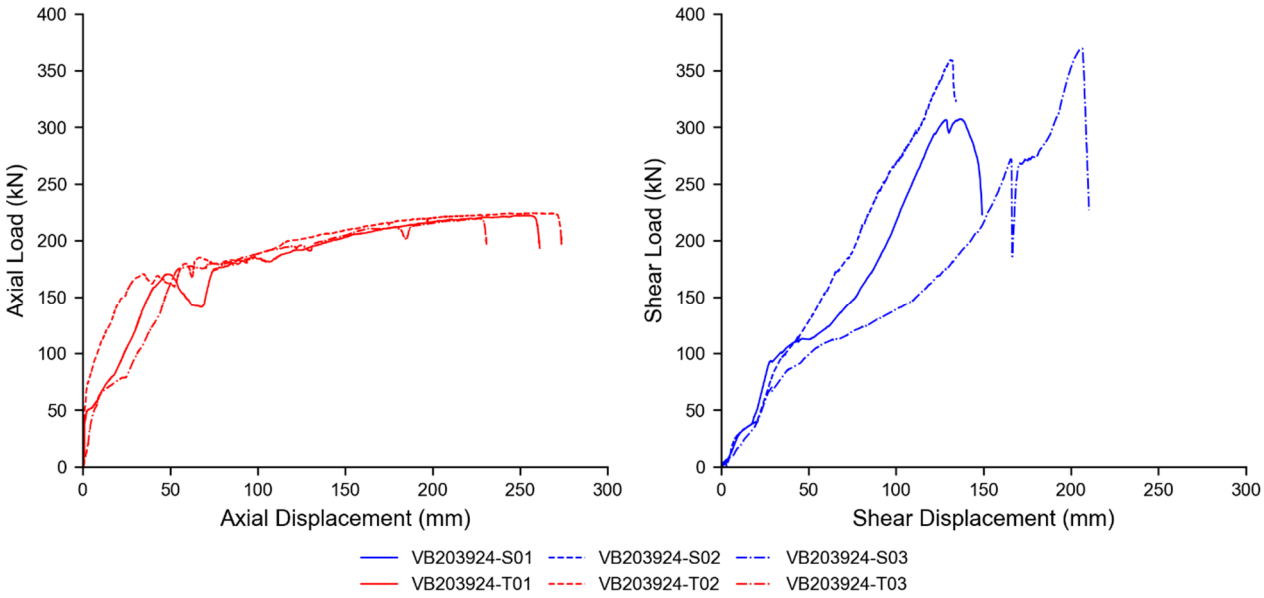

Figure 10 Load–displacement response of the mechanical hybrid rockbolt under axial and shear loading cases

Figure 11 Condition of friction unit after axial loading and rupture of the bar

In Figure 12, the significant deformation of the plate loaded on an irregular surface is observed. While the loading interface was irregular, the spherical seat did not ‘pull through’ the plate. This is significant as the spherical seat provides the load transfer mechanism between the plate and the nut. Pulling through would constitute a failure of the system.

The shear interface photographed after rupture of the samples is shown in Figure 13. The horizontal width of the fractured concrete for sample VB-203924-S03 was 230 mm. Fracturing of the concrete around the boreholes was evident during the shear loading of samples S01 and S02. Fracturing was only apparent at approximately 165 mm for sample S03 and may have contributed to the loss of shear load recorded in the testing results.

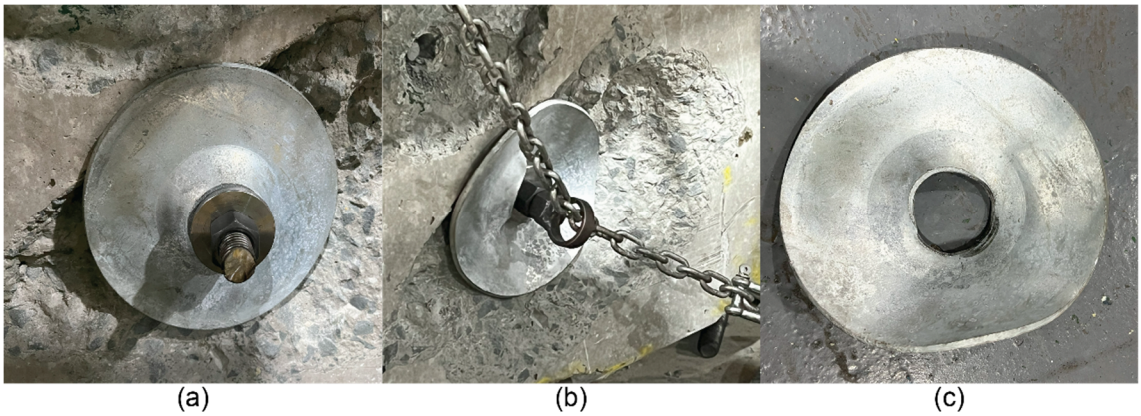

Figure 12 Response of the washer during loading on an irregular surface. (a) Setup; (b) During axial loading; (c) Post-axial loading

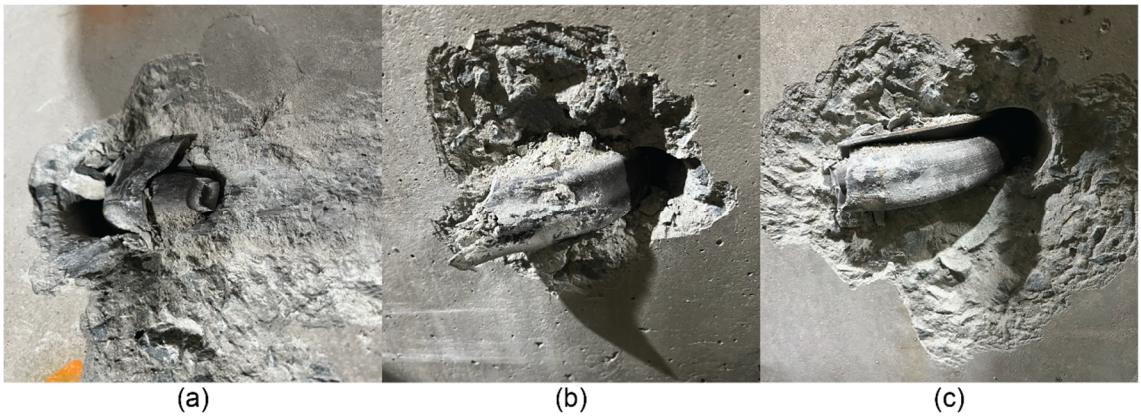

Figure 13 Comparison of the shear rupture interface. (a) VB-203924-S01; (b) VB-203924-S02; (c) VB-203924-S03

Another objective of the experimental program was to compare the axial and shear loading capacity of the mechanical hybrid rockbolt (Table 3). The average shear load capacity of the mechanical hybrid rockbolt was 55% greater than the average axial capacity recorded.

Table 3 Average results for the pull testing

Loading direction	Loading angle	Avg. $\delta_{A_{UF}}$ (mm)	Avg. $F_{A_{max}}$ (kN)	Avg. $\delta_{s_{UF}}$ (mm)	Avg. $F_{s_{max}}$ (kN)	$\frac{Avg.\ F_{s_{max}}}{Avg.\ F_{t_{max}}}$	$\frac{\delta_{s_{UF}}}{\delta_{t_{UF}}}$
Axial	0°	246	222	–	–	1.55	0.64
Shear	90°	–	–	158	345		

5 Analysis and interpretation of the results

As the mechanical hybrid rockbolt does not rely on a chemical agent for its reinforcement action, loading is applied directly between the mechanical wedge anchor and the plate. Consequently, the total axial capacity of the tendon is applied through the plate. Thus the interaction between the spherical seat and the plate is of importance. During these tests it was observed that the spherical seat did not pull through the plate during loading. Significant deformation of the plate was observed during the loading on an irregular loading surface.

While the FRS component of the mechanical hybrid rockbolt may have contributed to the total axial load capacity during the first 50 to 100 mm of axial displacement, the loads recorded beyond 100 mm are typical of the anticipated tendon loads. The profile of the borehole was both stable and oversized. In practice, in

heavily fractured rock masses the movement of the rock mass around the borehole will potentially result in mechanical interlocking, increasing the contribution of the FRS component of the mechanical hybrid rockbolt.

Shear loading of the mechanical hybrid rockbolt was successfully completed. The loading of all three samples (S01 to S03) resulted in the rupture of both the tendon and the FRS. The shear loading resulted in the two components being loaded in parallel and an average ultimate shear load 345 kN, which was greater than the average ultimate axial load of 222 kN. The difference in recorded load between the two loading cases can be attributed to the tendon rupturing independently of the FRS during axial loading. Samples S01 and S02 recorded similar shear displacements at peak load – 136 and 131 mm, respectively – while S03 recorded a higher shear displacement capacity of 206 mm.

Also observed in post-test photos (Figure 13) and during the analysis of the shear samples, the 'c-shape' of the FRS had collapsed. This phenomenon and the absence of a chemical anchor contributed to the observed shear displacements.

The relative higher shear resistance of the mechanical hybrid rockbolt, when compared to its tensile capacity, is of significance. This is consistent with the behaviour of FRS (Stjern 1995), but not with rebar bolts (Chen & Li 2014). This discrepancy emphasises the need for specific shear resistance testing for mechanical hybrid rockbolts as opposed to extrapolating from other tests of similar rockbolts.

6 Conclusion

Recent years have seen an increase in the application of mechanical hybrid rockbolts as part of ground support systems in poor ground conditions. Previous laboratory investigations into the performance of mechanical hybrid rockbolts had focused on axial plate loading conditions. These conditions, however, load the tendon independently of the friction unit and do not capture the frictional resistance offered by the total length of the FRS element of the rockbolt. In this investigation a joint was placed approximately at the mid-point of the rockbolt. Subsequently the FRS and tendon elements were loaded during the axial loading condition. An average displacement of 246 mm at a maximum load of 222 kN was recorded.

A series of successful shear tests of a mechanical hybrid rockbolt were conducted, providing the first published results for the rockbolt type. An average shear displacement of 158 mm at a maximum load of 345 kN was recorded. Therefore, the average maximum shear load recorded was higher than the average tensile load recoded with a relationship 1.55 ($F_{s_{max}}/F_{A_{max}}$). The average displacement at peak load of 158 mm in shear loading was less than the displacement of 246 mm recorded during axial loading, resulting in a relationship of 0.64 ($\delta_{s_{UF}}/\delta_{A_{UF}}$). These results provide valuable insights into the relative performance in shear of mechanical hybrid bolts compared to other rockbolts.

Acknowledgement

The authors acknowledge Epiroc for providing access to the testing facility and the Vulcan Bolts used in this testing campaign. The contribution of Lwazi Pambuka and his team in operating the testing facility is gratefully acknowledged. The support of the Natural Sciences and Engineering Research Council of Canada is acknowledged.

References

Andrews, PG 2019, 'Ground support selection rationale: a Gold Fields perspective', in J Hadjigeorgiou & M Hudyma (eds), *Ground Support 2019: Proceedings of the Ninth International Symposium on Ground Support in Mining and Underground Construction*, Australian Centre for Geomechanics, Perth, pp. 15–28, https://doi.org/10.36487/ACG_rep/1925_0.02_Andrews

Bray, P, Johnsson, A & Schunnesson, H 2019, 'Rock reinforcement solutions case study: Malmberget iron ore mine, Sweden', in W Joughin (ed.), *Deep Mining 2019: Proceedings of the Ninth International Conference on Deep and High Stress Mining*, The Southern African Institute of Mining and Metallurgy, Johannesburg, pp. 191–204, https://doi.org/10.36487/ACG_rep/1952_15_Bray

Chen, Y & Li, C 2014, 'Performance of fully encapsulated rebar bolts and D-Bolts under combined pull-and-shear loading', *Tunnelling and Underground Space Technology*, vol.45, pp. 99–106.

Darlington, B, Rataj, M, Balog, G & Barnett, D 2018, 'Development of the MDX Bolt and in-situ dynamic testing at Telfer Gold Mine', *Rock Dynamics and Applications,* CRC Press, Boca Raton.

Darlington, B, Rataj, M & Roach, W 2019, 'A new method to evaluate dynamic bolts and the development of a new dynamic rock bolt', in W Joughin (ed.), *Deep Mining 2019: Proceedings of the Ninth International Conference on Deep and High Stress Mining*, The Southern African Institute of Mining and Metallurgy, Johannesburg, pp. 205–216, https://doi.org/10.36487/ACG_rep/1952_16_Darlington

DSI Underground 2023, *KINLOC® Bolt*, viewed 2 February 2023, https://www.dsiunderground.com.au/products/mining/rock-bolts/friction-bolts/kinloc

Epiroc 2023, *Vulcan Bolt*, viewed 2 February 2023, https://www.epiroc.com/en-ba/products/rock-drilling-tools/ground-support/energy-absorbing-rockbolts/vulcan-bolt

Hartmann, W & Hebblewhite, B 2003, 'Understanding the performance of rock reinforcement elements under shear loading through laboratory testing - A 30 year history', *Proceedings of the 1st AGCM Conference*.

Jennmar 2023, *Mech Lok Bolt*, viewed 2 February 2023, https://www.jennmar.com.au/assets/Uploads/Documents/Hard-Rock-Catalogue-Feb-2021/MM-B-JML4724G.pdf

Knox, G & Hadjigeorgiou, J 2023, 'Performance of conventional and energy-absorbing self-drilling hollow core rock bolts under controlled laboratory conditions', *Rock Mech Rock Eng*, vol. 56, pp. 4363–4378.

Roach, W, Rataj, M & Darlington, B 2019, 'Development of a new Sandvik 'little brother' dynamic rockbolt and the in situ dynamic evaluation of bolts', in J Hadjigeorgiou & M Hudyma (eds), *Ground Support 2019: Proceedings of the Ninth International Symposium on Ground Support in Mining and Underground Construction*, Australian Centre for Geomechanics, Perth, pp. 201–212, https://doi.org/10.36487/ACG_rep/1925_12_Roach

Sandvik 2023, *The MDX Bolt*, viewed 2 February 2023, https://www.rocktechnology.sandvik/en/campaigns/the-mdx-bolt/

Stacey, T 2012, 'A philosophical view on the testing of rock support for rockburst conditions', *Journal of the Southern African Institute of Mining and Metallurgy*, vol. 112, no. 8, pp. 1–8.

Stjern, G 1995, *Practical Performance of Rock Bolts*, PhD thesis, Norwegian University of Science and Technology, Trondheim.

Turcotte, P 2010, 'Field behaviour of hybrid bolt at LaRonde Mine', in M Van Sint Jan & Y Potvin (eds), *Deep Mining 2010: Proceedings of the Fifth International Seminar on Deep and High Stress Mining*, Australian Centre for Geomechanics, Perth, pp. 309–320, https://doi.org/10.36487/ACG_repo/1074_22

Vallati, O, Darlington, B & Sandberg, L 2022, 'Dynamic drop testing of Sandvik's D47 and D39 MDX bolts at the Swerim's testing facility', *Proceedings of The Fifth Australasian Ground Control in Mining Conference Proceedings*, Australasian Institute of Mining and Metallurgy, Melbourne, pp. 428–440.

Watt, G, Roberts, T, & Faulkner, D 2018, 'Single pass drill, install and inject self-drilling resin bolt applications in poor ground', *Proceedings of The Fourth Australasian Ground Control in Mining Conference Proceedings*, Australasian Institute of Mining and Metallurgy, Melbourne, pp. 323–343.